Search for Sulfur Emissions at Jupiter's Moon Europa

Addi Djikic & Lukas Bjarre

***Abstract*—The objective of this research was to find sulfur emissions in the atmosphere of Jupiter's Galilean moon Europa. Sulfur is an ample element of life and therefore beneficial to science research for the potential in finding living organisms. The process began with collecting, analysing along with extracting spectral data taken from NASA's Hubble Space Telescope (HST), with the Cosmic Origins Spectrograph (COS) attached to the HST. In order to analyse the data, a spectrum of sunlight from the SUMER spectrograph was removed to see only the contents originating from Europa's atmosphere. The conclusion was that no sulfur emissions could be seen from the given data and therefore no evidence of sulfur could be deduced. However, there have been previous detections of some sulfur at Europa, and perhaps future research will disclose whether it exist or not. The report will present how the conclusion was made and how future research in the area could help to find more evidence of sulfur traces.**

I. Introduction

EUROPA is one of the four Galilean moons orbiting Jupiter, discovered in 1610 by Galileo Galilei, and is somewhat smaller than Earth's moon [1]. It is known that Europa is covered with a relatively smooth surface of ice with an ocean beneath it. NASA suspects that Europa has an iron core alike our planet [1], and that volcanic activities at the ocean floor could lead to sulfur abundance in the atmosphere.

A. Finding sulfur

The intention to study sulfur (atomic symbol S) is by reason of life. When in search for life it is first determined what life forms are in need of, and some basic substances are water, carbon, phosphorus nitrogen and sulfur, described in [2] and [3]. There are also several amino acids and compounds found in mammal tissues where the main ingredient is sulfur [4]. Therefore the confirmation of sulfur emission existence in both Europa's and other planets atmosphere could be significant in the pursuit of extraterrestrial life.

B. Liquid water

One explanation of the liquid ocean beneath the ice is due to a phenomena called tidal heating, explained by [5]. Europa is, as our moon to Earth, tidal locked to Jupiter [6]. The Galileo Spacecraft has been orbiting Europa and the spacecrafts magnetometer has shown no evidence that Europa contains an internal magnetic field [5], but instead an external magnetic field induced by Jupiter's Jovian magnetosphere. These electromagnetic events are result of conductivity within the moon, and therefore the most possible explanation is conductive salt water according to [5]. This is also what NASA explains in their Europa In Depth-article [1].

C. Previous detections of sulfur

Traces of sulfur have been found in previous analyses, for instance [7] mentions that ionized sulfur with S^{+}, S^{++} and S^{+++} occurring approximately in the same amounts but not in great quantity. NASA also mention it in [8] that sulfur exists in the ice of Europa. We already know the atmosphere is amply with oxygen [7], [9]. Previous research has shown that oxygen ions outnumber the sulfur ions roughly 5 to 1, with some variation in time and position on Europa [7]. This would lead to very low traces of sulfur, which of course makes the detection more difficult.

Previous research could point towards three different explanations for the presence of sulfur:

1) Sulfur originating from Io: The above mentioned sulfur ions found in Europa's atmosphere could originate from its neighbour Galilean moon Io [8], which have some similarities with Europa. The sulfur comes from Io's volcanoes and becomes ionized in the atmosphere and later transported to Europa where it gets encapsulated in the ice. It could be the only trace of sulfur that exist on Europa, and not come from Europa's ocean itself.

2) Releasing sulfur from the ice: Different atoms are affected and released by the Jovian magnetosphere of Jupiter [10], [11]. For most part the magnetosphere of Jupiter impacts Europa with electrons that hit the ice and therefore atoms, mostly hydrogen and oxygen are released and sent into the atmosphere. The heavier atoms are left in the atmosphere but the lighter, mostly hydrogen are sent into space. This is also the explanation why Europa's ionosphere is rich with oxygen, and how sulfur emission may have been released.

3) Water plumes arising from the ice crust: Observations at the south pole of Europa back in 2012 have shown water plumes arising as high as 200 km above the surface via cracks in the ice [12]. If sulfur is abundant under the ice crust, this could be a way for the sulfur to arise into the atmosphere.

D. The Hubble Space Telescope & Cosmic Origins Spectrograph

The data collection used in this research is from NASA's Hubble Space Telescope (HST) [13], captured with a particular camera attached to it, the Cosmic Origins Spectrograph (COS) [14]. The COS was installed to the HST in 2009 to study large scale origins of the universe. The COS features a more sensitive ultraviolet (UV) sensors compared to older cameras on the HST, making it more capable to detect more faint emissions in the UV spectrum [14]. This will be important to find excitations of sulfur atoms in the interesting part of the

spectra. The COS has a field of view of 2.5 arcsec in aperture [15]. The COS includes a far ultraviolet (FUV) detector which is used to study wavelengths at the range of 900-2150 Å and a near ultraviolet (NUV) detector to study ranges of 1650-3200 Å. The COS-handbook [16] was used to understand how to handle the data via Flexible Image Transport System (FITS) files [17], often used for astronomical research purpose.

II. Theory

A. Atom excitations

When atoms undergo changes of energy states they release photons from the transitions. Depending on the energy transition different energetic photons are released, that is, photons of different wavelength. With several different energy states depending on the atom, every atom has its own fingerprint spectrum of different emission lines caused by the excitations. By identifying these emission lines from spectrum analysis of incoming photons, atoms from distant places can be found.

1) Sulfur emission lines: Sulfur has, as other elements, a set of unique wavelengths emissions when excited. An analysis were made by Roesler et. al. [18] on the neighbour moon Io. They plotted an intensity plot of the FUV spectrum, see Fig. 1, that includes wavelengths for emission lines of several elements, including sulfur. If sulfur was present in a spectrum, some amount of intensity in these wavelengths is expected.

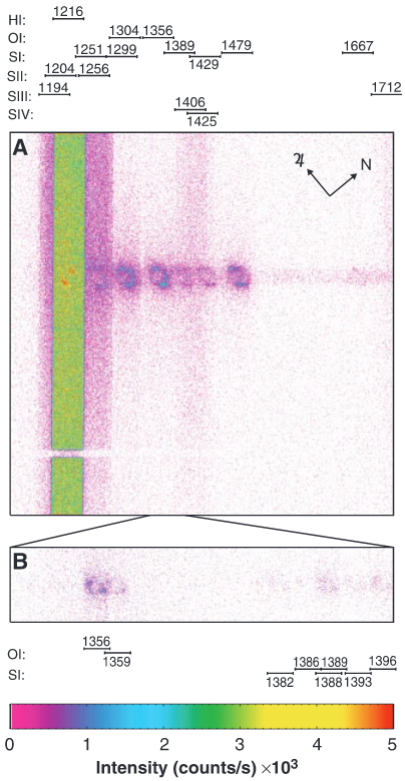

Fig. 1. Image taken from Roesler et. al. [18], which displays an intensity plot of the neighbouring moon Io in the far ultraviolet (FUV) spectrum. It also shows the wavelengths in Ångströms of emission lines for several elements, including sulfur.

B. Spectrography

The method of gathering information from Europa is by spectrography. By dispersing incoming light into different wavelengths one can study its contents according to the theory described in section II-A.

C. Solar light reflection on Europa

The difficulty with determining different atoms in the visible UV spectrum is due to background noise and other disturbances. Most reflected light on Europa originates from the Sun and stand for the majority of this disturbance. Solar light will add up on the emission spectra from Europa, making it impossible to differentiate between spectral contents from the Sun and from Europa. Therefore, to analyse the spectral contents of Europa the solar spectrum needs to be subtracted from the total spectrum.

1) Spectral atlas of the sun: In the paper by Curdt et al. [19], they give the whole far ultraviolet and extreme ultraviolet (EUV) spectral atlas of the solar disk in the range 670 Å to 1609 Å. With the diffracted atoms and ions from the spectrum captured by the SUMER (Solar Ultraviolet Measurements of Emitted Radiation) spectrograph [20]. These spectrum lines given by [19] can be used to compare the spectrum lines given by the extracted data from the COS. The solar atlas spectrum is then used to exclude the atoms and ions that comes from the sun and not Europa by appropriately scale and subtract the SUMER plots as described in Cunningham et. al. [21].

2) SUMER: Given the spectrum lines in Fig. 2 taken by the SUMER spectrograph from the spacecraft SOHO (Solar and Heliospheric Observatory) [19], [20]. That is later used to subtract from the spectrum lines intercepted by the COS-camera's FUV-detector as mentioned above.

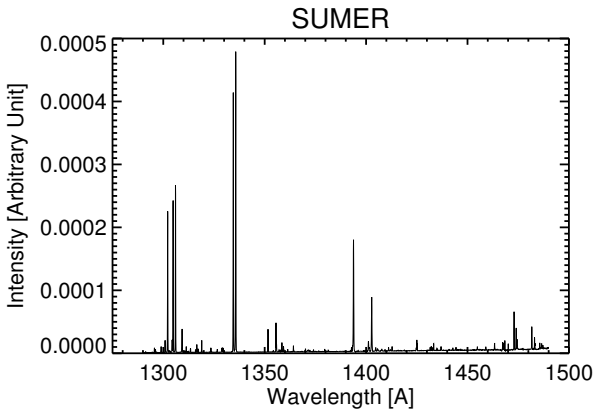

Fig. 2. Graph showing the solar spectrum taken by the SUMER. The intensity of the spectral lines, the y-axis, is not set in actual physical units but rather given as an arbitrary unit. This is intended to be scaled for the needed use, in the case of this research to match the reflected sunlight on Europa.

D. Doppler shift

The light observed from Europa has been distorted slightly by Doppler shift, caused by the relative motions of Europa, Jupiter and Earth. The Doppler shift between observed wavelength λ_o and source wavelength λ_s in a scenario with the

source moving relatively to the observer with speed $v \ll c$ is given by (1):

$$\lambda_o = \frac{1}{1 + \frac{v}{c}} \lambda_s \tag{1}$$

Calculating the exact Doppler shift for the exposure time requires detailed knowledge of the celestial bodies positions and relative speeds. A model of this seemed unnecessary for the project, talked about in section V-B2, so only an average shift from Europas orbital speed given by [22] was calculated.

E. Spectral data

The FITS-files used for the project where taken from Mikulski Archive for Space Telescopes (MAST) [23]. Each recorded exposure consists of multiple files with data corresponding to smaller steps in the data calculation of the COS. The files interesting for this project where the extracted one-dimensional spectra files, marked with the suffix `x1d`. The used exposures consisted of several shorter exposures, which are in turn used to find statistical outliers in the data. These are removed in a final summation file, marked with the suffix `x1dsum`. The `x1dsum`-files were the ones used for this project.

Each file includes a header file consisting of various information parameters of the data, like exposure date, the range of observed wavelength, and the platescale (arcseconds per pixel). The description of the parameters and how they were used was described in the COS-handbook [16], including the information about the A and B central wavelengths parts (1327 Å) of the spectrum. All from the spectral resolution G130M-table given in [16]. This is where the interesting parts of the spectrum is, that is, the FUV-range. The files also includes several different data sets for different observed data. The ones interesting for the project were the photon flux and estimated error, both given in $[\mathrm{erg\ s^{-1}cm^{-2}A^{-1}}]$.

III. Method

A. Data extraction and plotting in IDL

Data sets from two exposures were used, `lcnr01010` and `lcnr01020`, both taken by the COS on board the HST and downloaded via MAST [23]. General information about the different exposures can be found in Table I.

TABLE I
EXPOSURE DATA

	`lcnr01010`	`lcnr01020`
Observation date	2015-12-03	2015-12-03
Observation start	01:36:50	04:59:52
Exposure time [s]	5590.976	6130.336
FUV Grating	G130M	G160M
Wavelengths in segment B [Å]	1172 - 1313	1397 - 1571
Wavelengths in segment A [Å]	1328 - 1469	1589 - 1762

The FITS-files were then handled with the Interactive Data Language (IDL) [24] for data manipulation and visualization. An Gaussian smooth function was directly applied to the data to reduce the noise present in the spectrum. An example of the used data can be seen in Fig. 3, where the A segment of the `lcnr01010`-exposure is plotted.

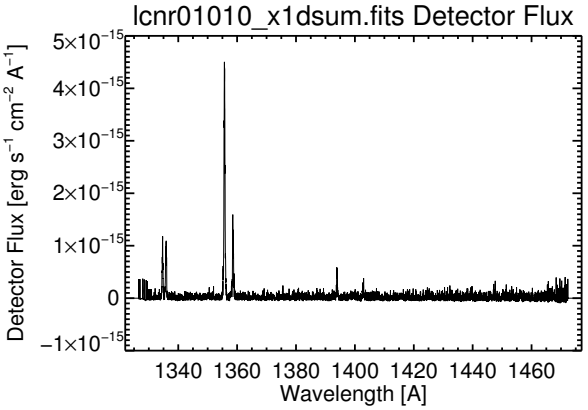

Fig. 3. Detector flux from the A segment of the `lcnr01010`-exposure.

B. Solar subtraction

When comparing the spectrum spikes in Fig. 3 with the solar spectrum lines given by the SUMER in Fig. 2 [19], several large peaks were found in both spectra; the carbon-doublet (C-II) around 1335 Å, oxygen (O) around 1355 Å and silicon (Si) near 1394 Å. A large spike near 1216 Å was present in the B-spectrum of the `lcnr01010` from the Lyman-α emission. From a first observation it seemed clear that the COS spectra contains reflected sunlight which needed to be subtracted in order to only look at the atom excitations from Europa. When the SUMER- and the `lcnr01010`-spectra were plotted on top of each other, a small but clear Doppler shift was visible as seen in Fig. 4 which also needed to be considered for the subtraction.

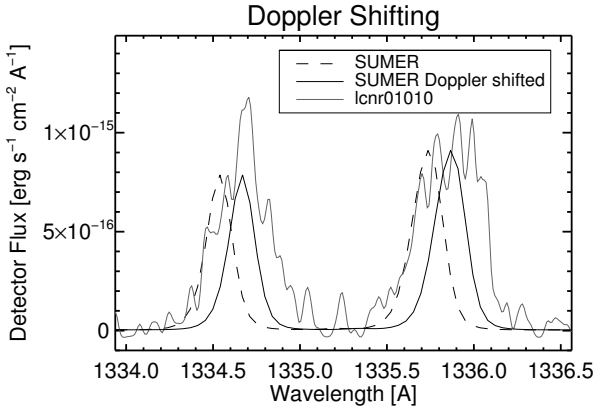

Fig. 4. Detector flux from `lcnr01010` and the solar spectrum from SUMER around 1335 Å. The doppler shift of the spectrum taken from the COS can be clearly viewed in this example. The dashed lines view the SUMER spectrum before the Doppler shift was adjusted for, and the whole drawn line after a shift of 0.14 Å was applied.

1) Scale factor of solar spectrum: As described in Fig. 2, the solar spectrum given by [19] was given in an arbitrary unit that needed to be scaled until it coordinated with the

same intensity of the emission lines from the lcnr01010-exposure. This was done with the emission lines around the doublet C-II emission peaks at 1335 Å in accordance to [21]. The higher wavelength peak of the SUMER spectrum was scaled until it matched the one from the COS spectrum. This left the lower wavelength peak from the COS spectrum larger than the one from the SUMER spectrum, something that could mean that a section of that peak originates from Europa itself.

2) Doppler shifting: The Doppler shift was estimated according to (1), where the average orbital speed of the Earth were taking account to and the average orbital speed of Europa found in [22], although the celestial bodies position relative to each other makes them behave differently. For instance, when Europa is moving away from Earth or towards it and vice verse would create Doppler shifts in different directions. Since creating an exact model for the relative motion between Europa and Earth would be difficult and tedious, an idealised case was used for the Doppler calculation. Assuming that Europas orbital path is radially aligned towards Earth and using the average orbital speed of Europa yields a Doppler shift estimation of ± 0.14 Å. This did a small but not negligible effect to the spectrum. Furthermore, the adjustment of the shift was also done according to [21], where the SUMER spectrum was shifted until the doublet C-II peaks around 1335 Å aligned. Fig. 4 shows both the SUMER spectrum and the lcnr01010-exposures spectrum plotted in one graph around the C-II peaks. A shift in wavelengths of 0.13 Å was measured between these peaks, a Doppler shift which lies very close to the idealised model. This measured shift of 0.13 Å was applied to the SUMER spectrum in order to align it with the COS spectra.

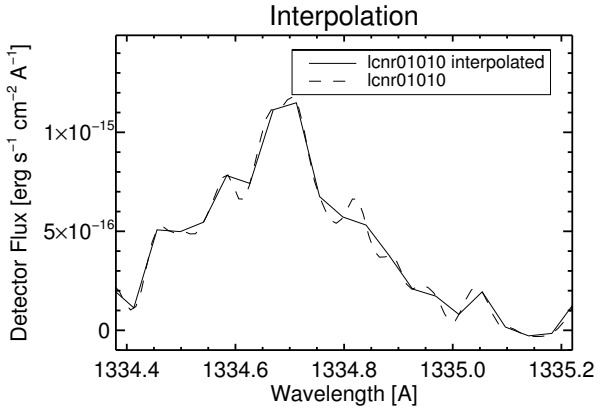

Fig. 5. The lcnr01010 spectrum before and after the linear interpolation was applied. A very small reduction in resolution can be seen, but these are small compared to the size of the emission line.

3) Interpolation with the total solar spectrum: When aligning the final Doppler shifted spectral resolution of both the solar atlas and the x1dsum, there was a difference between the sampling points of both the spectra. When all wavelengths of the G130M were included and the whole SUMER spectrum, then IDL gave an output that the COS spectra was 16384 sample points (measured in different wavelengths) and the SUMER was 4706 sample points. When subtracting the solar spectrum from the COS spectra with a different sample rate, it would be problematic if the wavelengths did not align at the same points, thus it was necessary to first down-sample the COS spectra to the corresponding SUMER spectrum. This was done by linear interpolation with the COS-data in correlation with the SUMER-data by IDL. An example of the interpolated spectrum can be seen in Fig. 5. Even though some of the spectral resolution was lost after the downsample it was low compared to the rest of the spectrum. Therefore the spectral resolution was deemed to be good enough for the primary data to be analysed.

4) Spectral width: The final step needed before subtracting the interpolated spectrum from the COS spectra were to consider the width of the emission lines in the solar spectrum. Overlapping sample points from the COS spectra makes the emission lines wider compared to the ones from the SUMER spectrum. In order for the SUMER spectrum to fully align with the COS spectra a Gaussian smoothing function was applied to the SUMER spectrum with a σ of 3.8, which as seen in Fig. 6 made the peaks in both spectra similarly broad.

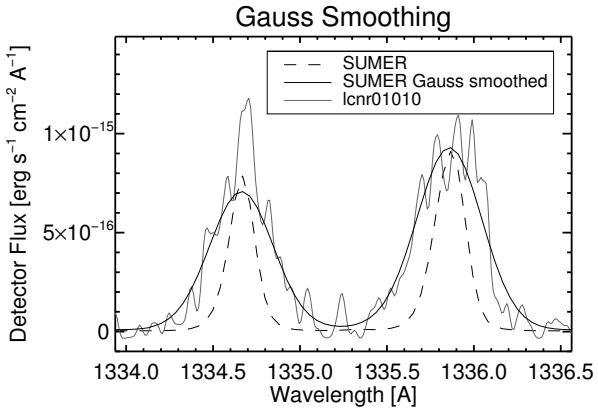

Fig. 6. Graph showing the SUMER spectrum before and after the Gaussian smoothing, displayed in the dashed and whole curves respectively. The spectrum after the smoothing closely follows the COS spectrum around the C-II peaks around 1335 Å, shown in lighter grey.

5) Final subtraction: After all steps above were applied to the SUMER spectrum it could be removed from the spectra taken from the COS. Fig. 7 shows the result around the C-II peaks around 1335 Å for the lcnr01010-exposure.

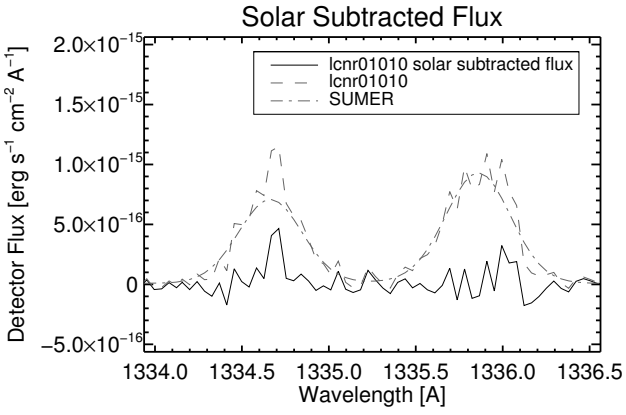

Fig. 7. The C-II peaks after subtracting the adjusted solar spectrum.

C. The 1356/1304 Å ratio

Europa's rich O_2 atmosphere were officially determined in 1995 by [10] with the discovery of a triplet oxygen emission line around 1304 Å and a doublet oxygen emission line around 1356 Å. Both [10] and [21] speaks about that the ratio on the amount of oxygen between 1356 and 1304 Å should be abide by as 2:1. As a result of that these peaks are established and unchanging, the area around 1356 Å was integrated with help of IDL as well as the 1304 to determine the ratio for this case. After integration and division of the spectra areas were made it yield the result 0.37 (1356/1304). This was probably due to that the O-I at 1304 was increased by the light from Earth's geocorona. Therefore, the ratio is not representative of only Europa emissions.

D. Standard deviation error

As described in section II-E, each `x1dsum`-file from the exposures featured a standard deviation error σ for each sampled wavelength, calculated by the COS from the multiple smaller exposures and background spectrum. σ of the A segment from the `lcnr01010`-exposure can be viewed in Fig. 8. It seems from the graph that the flux near the edges of the observed wavelengths are less reliable, and an overall tendency of a larger σ for higher wavelengths.

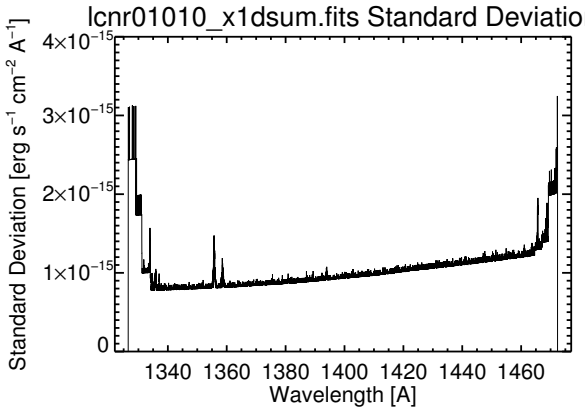

Fig. 8. The standard deviation of the detector flux from the A segment of the `lcnr01010`-exposure.

The standard deviations were given for each discrete sample point in the spectrum. However, since the final values used were integrated over multiple sample points, every σ across this range needed to be considered for a total standard deviation σ_{total}. For a range of wavelengths from n to N, σ_{total} was calculated with (2).

$$\sigma_{total} = \frac{\sqrt{\sigma_n^2 + \sigma_{n+1}^2 + \sigma_{n+2}^2 + \ldots + \sigma_N^2}}{N - n} \tag{2}$$

E. Unit conversion

1) Photon energy and scale factors: The final part of the data analysis were to convert the photon flux to the more conventional unit, rayleigh [R], or $[10^{10}\ \mathrm{s^{-1}m^{-2}}]$. The unit given from the COS data, $[\mathrm{erg\,s^{-1}cm^{-2}A^{-1}}]$, is already close to the final unit with the only difference being the wavelength in the denominator, the energy in the numerator, and some scale factors. The energy of the incoming photon was expressed by (3), where h is Planck's constant, c the speed of light and λ the wavelength of the photon.

$$E = \frac{hc}{\lambda} \tag{3}$$

Two additional scale factors needed to be considered in (3), since the COS use erg $[10^{-7}\ \mathrm{J}]$ and Å $[10^{-10}\ \mathrm{m}]$ instead of the standard SI units. The unit from COS also uses cm^2 in the denominator, which needed to be taken into account and rescaled. Adding all the scale factors together gives a final factor of 10^{-12}, which were added to (3) and divided from the detector flux.

2) Integration over wavelengths: Finally, to remove the wavelength in the denominator the detector flux curve was integrated over the excitation peaks of interest in the spectra. Ideally the entire emission line of interest should be integrated over to ensure that the spectral resolution is considered when counting the photon flux. However, the sought emission lines where not always apparent in the spectrum which made the desired $\Delta\lambda$ region of integration difficult to determine. Other more visible emission lines, like the O-I line at 1356 Å in Fig. 9, were investigated to conclude that a $\Delta\lambda$ of 1 Å seemed to fit the spectral resolution of the spectra. This also had the added benefit of not needing any more scale factors since the integration distance always was 1 Å.

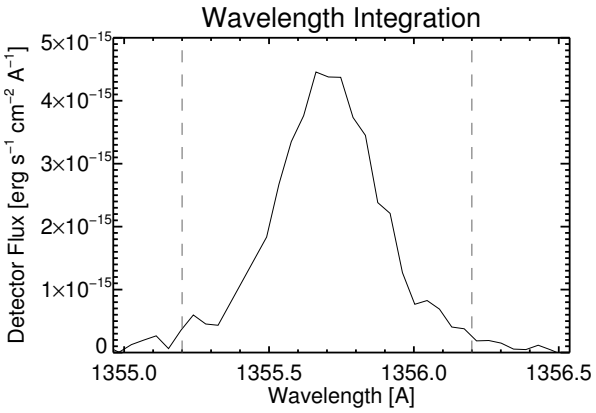

Fig. 9. Graph showing the O-I emission line near 1356 Å, taken from the `lcnr01010`-exposure. The two dashed lines represents a $\Delta\lambda$ of 1 Å as described in section III-E2, which is seen here to neatly fit the entire emission line. This measure was used for other parts of the spectrum where the emission line was not as apparent as in this case.

F. Wavelengths of interest

As mention in section II-A1, Roesler et. al. [18] presented some interesting wavelengths where possible sulfur emission could be found. The particular wavelengths for sulfur emission lines is visualized in Fig. 1. The brightness of these wavelengths in the solar subtracted spectra with converted units was measured by integration over the specified wavelength ± 0.5 Å as described in section III-E2. This procedure was repeated over all the wavelengths corresponding to sulfur emissions

from Fig. 1 which is present in the given spectra from the lcnr01010- and lcnr01020-exposures.

IV. Results

Table II shows the calculated brightness in milli-rayleigh of the different sulfur emission lines seen in Fig. 1 and present in the exposures.

TABLE II
SULFUR BRIGHTNESS

Wavelength [Å]	Brightness [mR]	
	lcnr01010	lcnr01020
1299	23.9 ± 89.5	N.A.
1389	16.7 ± 126	N.A.
1406	18.4 ± 140	8.59 ± 98.1
1424	43.6 ± 152	9.18 ± 103
1429	16.3 ± 154	1.77 ± 104
1479	N.A	3.46 ± 133

None of the results from Table II had a measured brightness larger than the accompanied σ_{total}, which would suggest that all of the points of interest only contain noise. This is further confirmed by looking at the spectrum, as done for the lcnr01010-exposure at 1429 Å in Fig. 10. The measurement with the smallest uncertainty is the 1299 Å emission line from the lcnr01010-exposure, and although the σ_{total} is larger than the measured brightness, it is the only result in which the two values are in the same order of magnitude. The results from the lcnr01020-exposure seems to be smaller than the ones from the lcnr01010-exposure, as evidently seen in the overlapping results from the 1406 Å, 1424 Å, and 1429 Å emission lines. This could possibly be because of the different FUV gratings used in the exposures. As the data suggests, there is no evidence of sulfur emissions in the given exposures.

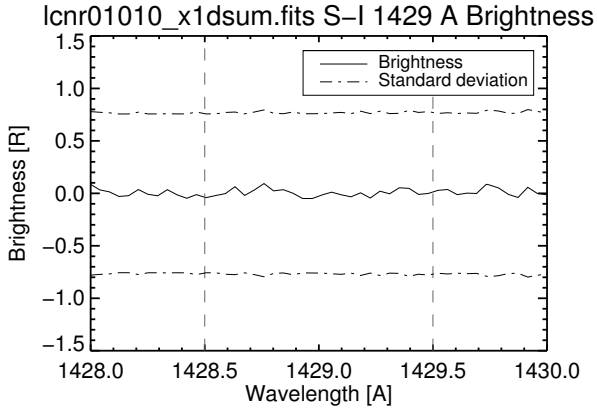

Fig. 10. Brightness and standard deviation from the lcnr01010-exposure with the adjusted solar spectrum subtracted around the S-I emission line at 1429 Å. Even with no background noise subtracted it can clearly be seen that only noise is present in this part of the spectrum.

V. Discussion

A. Method of spectrography

The proceedings of this study on the moon Europa were mainly concentrated around spectrography methods. The main objective were to subtract as much of the unwanted data from the spectrum to get as a clear picture as possible of the interesting parts where sulfur may occur. One can argue that the methodology used for this analyse had insufficient mathematical reliability, for instance how the parameters and factors of the Gaussian smooth applied to the spectra. The implication is that this research is based much on empirical study with spectrum. One could instead derive the exact Doppler shift and calculate all factors of the Gaussian smooth that broaden the line and generate a reflection spectrum. In other words, do the computations more exact by applying more methods and mathematical calculations, but it may not be certain if it will make any major difference for the result.

B. Ignored data & errors

1) FITS-background & sky disturbance: The dominant error, or unwanted data, in the case for the COS data was from the solar-atlas reflections on the moon. Nevertheless, considering the COS data given, with including background error in the given FITS-files, and the sky background disturbance of both the Europa and Earth, there are more disturbance that exists. For instance, if the HST was affected by the Earth's atmosphere and if the data were captured in Earth's shadow or not is an example of sky background error from Earth. This tells that there is much more that could be excluded. The conclusion was that these type of errors mentioned, background error included in the FITS and the sky disturbance from Earth, could be omitted, thus they were negligible when compared to the SUMER data given by the solar-atlas.

2) Doppler shift error: For the compensation of the Doppler shift the average orbital speeds of the moon and Earth were used (see section III-B). Though the calculations was not necessarily needed because the shift was done manually with IDL with reference to 1335 Å according to [21]. It was still a relevant calculation to visualize the difference between the calculated value and the empirically reached value, which was very similar, in any case at least the same order of magnitude, which was very promising. If one desires a more refine result, the Doppler shift can be compensated by first finding out the exact speed and position of Europa and Earth relative to each other when the data exposure was captured.

C. Other methods than linear interpolation

The non equal sample points between the SUMER and the COS-data were an issue, and thereof interpolation was used to sample down the data points so that the SUMER was only subtracted from the irrelevant COS data. This sampling method may be the simplest and it is quite accurate too, but other methods could be used also. For instance there were first an attempt to find the equal points of the spectra's with help of

IDL, and then subtract those exact points. That method did not turn out to work entirely. Perhaps this could be endeavoured in future experiment.

D. Considering the interesting emission lines

In Fig. 10 together with Table II, there is a clear noise visible with a standard deviation error much bigger than the actual spectra, even though the solar-atlas spectra have been subtracted. Of course there could be other considerations to take into account as told in section V-B. In this case there were no visible sulfur emission lines in the 1429 Å and 1479 Å only noise left, yielding the expected result that no sulfur emissions were found in the other interesting wavelengths besides the 1429 Å and 1479 Å, given in Fig. 1. Thereof it may have been redundant to even check the area around those emission lines.

E. Low brightness at given sulfur emission lines

As seen in table II the brightness in milli-rayleigh are displayed along with the standard deviation of the brightness. The conclusion is that because of the extremely low brightness and the dominating error given, σ, it is almost certain that no sulfur emission may exists in these areas. When comparing with the previous years paper on the same research, "Search of Sulfur in the Atmosphere of Europa", [25], the rayleighs around 1479 Å stretch from 0.69 ± 1.98 R to 6.18 ± 1.93 R. Concluding that the rayleighs in Table II indicate much lower brightness emissions, giving a clearer result that no detectable sulfur emissions are present in this area.

F. Future improvements in same area of research

As discussed, other noise-canceling, or error-canceling methods may be applied to give a more accurate result, such as subtracting the unused image of the aperture and only use the aperture of Europa. This would exclude the majority of the sky-background noise. But the major improvements lies in gathering more data of Europa, for instance sending probes to the moon to get the whole perspective of the planetary satellite. But the improvements of today and near future lies in glancing at the moon until data of as much surface area as possible is collected throughout a longer period of time. Today the HST is used in many areas when looking into the vast universe. It is also used by many scientists, and thereof when gathering information about a planetary body there is not enough time to use the HST to get the complete data wanted of a moon for example. There is however, an alternative, and that is to create a simulation on the behaviour of the moon Europa and perhaps simulating sulfur emission excitations along with it. For the case, with the lack of time with the HST, it would be of great knowledge to know when the optimal time and place on the moon it would be most likely to see any sulfur abundance emerging from Europa.

VI. Conclusion

The conclusion for this research is that no detectable sulfur emission could be found on Europa in the given interesting spectrum with the data exposures. After working to exclude unnecessary data, the conclusion was more reliable and other additional methods of noise-cancellation were negligible. There is still room for future research in this area which will eventually yield in finding more evidence of sulfur on Europa than today.

Acknowledgment

The authors would like to give a special thanks to our supervisor Lorenz Roth for the guidance and time throughout the whole project. The authors would also like to thank NASA for making the data from the HST publicly available which allows research like this possible.

References

[1] B. Dunford and K. McKissick. (2016, Apr) Europa-In Depth NASA solar system exploration. [Online]. Available: http://solarsystem.nasa.gov/planets/europa/indepth

[2] C. P. McKay, "What is life—and how do we search for it in other worlds?" *PLoS Biol*, vol. 2, no. 9, p. e302, 2004.

[3] C. P., McKay, "Urey prize lecture: Planetary evolution and the origin of life," *Icarus*, vol. 91, no. 1, pp. 93–100, 1991.

[4] M. Gaitonde, "Sulfur amino acids," in *Metabolic Reactions in the Nervous System*. Springer, 1970, pp. 225–287.

[5] K. Khurana, M. Kivelson, D. Stevenson, G. Schubert, C. Russell, R. Walker, and C. Polanskey, "Induced magnetic fields as evidence for subsurface oceans in europa and callisto," *Nature*, vol. 395, no. 6704, pp. 777–780, 1998.

[6] ——. (2016, Apr) Tidal locking. [Online]. Available: https://en.wikipedia.org/wiki/Tidal_locking

[7] R. Johnson, M. Burger, T. Cassidy, F. Leblanc, M. Marconi, and W. Smyth, "Composition and detection of europa's sputter-induced atmosphere," *Europa, University of Arizona Press, Tucson*, pp. 507–527, 2009.

[8] E. Zubritsky. (2016, Apr) Europa's hidden ice chemistry. [Online]. Available: http://www.nasa.gov/topics/solarsystem/features/europa-ice_prt.htm

[9] M. McGrath, C. Hansen, and A. Hendrix, "Observations of europa's tenuous atmosphere," *Chapter in Europa. University of Arizona Press, Tucson*, vol. 85, 2009.

[10] D. Hall, D. Strobel, P. Feldman, M. McGrath, and H. Weaver, "Detection of an oxygen atmosphere on jupiter's moon europa." *Nature*, vol. 373, no. 6516, pp. 677–681, 1995.

[11] J. Saur, D. Strobel, and F. Neubauer, "Interaction of the jovian magnetosphere with europa: Constraints on the neutral atmosphere," *Journal of Geophysical Research: Planets*, vol. 103, no. E9, pp. 19 947–19 962, 1998.

[12] L. Roth, J. Saur, K. D. Retherford, D. F. Strobel, P. D. Feldman, M. A. McGrath, and F. Nimmo, "Transient Water Vapor at Europa's South Pole," *SCIENCE*, vol. 343, no. 6167, pp. 171–174, JAN 10 2014.

[13] K. Hille. (2016, Apr) NASA - Hubble Space Telescope. [Online]. Available: https://www.nasa.gov/mission_pages/hubble/main/index.html

[14] J. Debes et. al, *Cosmic Origins Spectrograph Instrument Handbook for Cycle 24*. Baltimore: Space Telescope Science Institute, 2016, vol. 8.

[15] ——. (2016, Apr) Minute and second of arc. [Online]. Available: https://en.wikipedia.org/wiki/Minute_and_second_of_arc

[16] A. J. Fox et. al, *COS Data Handbook*. Baltimore: Space Telescope Science Institute, 2015, vol. 3.

[17] ——. (2016, Apr) FITS. [Online]. Available: https://en.wikipedia.org/wiki/FITS

[18] F. Roesler, H. Moos, R. Oliversen, R. Woodward, K. Retherford, F. Scherb, M. McGrath, W. Smyth, P. Feldman, and D. Strobel, "Far-ultraviolet imaging spectroscopy of io's atmosphere with hst/stis," *Science*, vol. 283, no. 5400, pp. 353–357, 1999.

[19] W. Curdt, P. Brekke, U. Feldman, K. Wilhelm, B. Dwivedi, U. Schühle, and P. Lemaire, "The sumer spectral atlas of solar-disk features," *Astronomy & Astrophysics*, vol. 375, no. 2, pp. 591–613, 2001.

[20] L. Teriaca and U. Schühle. (2016, Apr) Instrumentation and data reduction. [Online]. Available: https://www2.mps.mpg.de/projects/soho/sumer/text/webluca/ch_inst.html

[21] N. J. Cunningham, J. R. Spencer, P. D. Feldman, D. F. Strobel, K. France, and S. N. Osterman, "Detection of callisto's oxygen atmosphere with the hubble space telescope," *Icarus*, vol. 254, pp. 178–189, 2015.
[22] C. J. Hamilton. (2016, Apr) Jupiter's Moon Europa. [Online]. Available: http://solarviews.com/eng/europa.htm
[23] ——. (2016, Apr) MAST. [Online]. Available: https://archive.stsci.edu/
[24] ——. (2016, Apr) IDL software - data visualization software. [Online]. Available: http://www.harrisgeospatial.com/ProductsandSolutions/GeospatialProducts/IDL.aspx
[25] O. Näslund and F. Ärlemalm, "Search of Sulfur in the Atmosphere of Europa," *Kandidatsexamensarbete*, vol. 1, pp. 143–149, 2015.